Experiments in machine learning of α -decay half-lives

Paulo S. A. Freitas¹ and John W. Clark^{2,3}

¹FCEE, Departamento de Matemática,

Universidade da Madeira, 9020-105 Funchal, Madeira, Portugal

²McDonnell Center for the Space Sciences & Department of Physics,

Washington University, St. Louis, MO 63130, USA

³Centro de Investigação em Matemática e Aplicações,

University of Madeira, 9020-105 Funchal, Madeira, Portugal

Abstract

Artificial neural networks are trained by a standard backpropagation learning algorithm with regularization to model and predict the systematics of -decay of heavy and superheavy nuclei. This approach to regression is implemented in two alternative modes: (i) construction of a statistical global model based solely on available experimental data for alpha-decay half-lives, and (ii) modeling of the residuals between the predictions of state-of-the-art phenomenological model (specifically, the effective liquid-drop model (ELDM)) and experiment. Analysis of the results provide insights on the strengths and limitations of this application of machine learning (ML) to exploration of the nuclear landscape in regions beyond the valley of stability.

1. INTRODUCTION

Machine learning has been applied to global statistical modeling and prediction of nuclear properties since the early 1990's [1]. Relative to phenomenology and fundamental theory, these studies have yielded complementary or competitive results for atomic masses, nucleon separation energies, charge radii, ground-state spins and parities, branching ratios, and beta-decay half-lives. Recently, this original wave has been followed up by a major surge of activity swept along by current enthusiasm for machine learning techniques across many scientific disciplines, notably in condensed matter physics and quantum chemistry (see especially Refs. [2–6], and work cited therein). Although there have been significant improvements in machine-learning techniques, the driving force has been the vast increase in computational power during the last two decades.

Modeling and prediction of α -decay observables of heavy nuclei has not received much attention within this thrust, past or present, although the study of superheavy nuclei, having Z > 104, remains an important dimension of experimental and theoretical study in expanding our knowledge of the nuclear landscape well beyond the familiar valley of stability [7]. Significantly, α decay and fission are the dominant modes of decay for this unique class of nuclei. Indeed, superheavy nuclei so defined are of special interest in that their existence is contingent on shell effects, giving rise to the "magic island" of nuclei enjoying relative stability. At this point, synthesis of many superheavy elements and isotopes has been achieved through cold, warm, and hot fusion, up to Z = 118.

Advances in fundamental understanding of the α -decay process date back to the fundamental breakthrough of Gamow and Condon and Gurney, who identified the underlying mechanism as quantum tunneling. Semi-empirical formulas have been introduced to estimate α -decay half-lives, such as that of Viola and Seaborg [8] and much more recently those of Royer [9] and Denisov [10]. However, apart from efforts toward true microscopic description of α decay, the current state-of-the art for its quantitative theoretical treatment resides in two phenomenological models based on semi-classical considerations. These are (i) the generalized liquid-drop model (GLDM) [11, 12], in fission-like and cluster-like modes, and (ii) the effective liquid-drop model (ELDM) [13, 14], together with their refinements. Among recent developments, see especially Refs. [15–17].

Past and recent efforts toward machine learning of α decay have been limited to Refs. [18,

19]. The first of these works was an exploratory study indicating that an artificial neural network approach to this problem domain may be successful. The second (which contains a very useful update of current ML activity in nuclear physics) concentrates on machine learning of the energy release Q_{α} , an essential input to calculation of α -decay half-lives.

Our aim in the present work is two-fold, namely to develop stand-alone statistical models for the α -decay process, with input limited principally to N, Z, and Q_{α} , and to refine the ELDM model by developing neural-network models of the residuals between this model and experiment. We begin with a brief introduction to machine learning, as realized by feedforward multilayer neural networks.

2. ELEMENTS OF STATISTICAL MODELING

Our objective is to use machine learning (ML) to model the mapping from the nucleonic content (N, Z) of a given nuclear species to the α -decay half-life $T_{1/2}$ of that nuclide, based on a set of experimental data that provides examples of this mapping. Since the goal is a real number rather than a correct choice among discrete outcomes, one is dealing with a task of regression (as opposed to classification), such that the problem may be formulated as follows.

The mathematical problem of approximating a function f that maps an input variable x to an output variable y may be expressed as

$$y = f(x, \theta; \Upsilon) + \epsilon, \tag{1}$$

with a set of data points (y_n, x_n) , $n = 1, ..., n_T$ (i.e., n_T given training "patterns") being made available for interpolation and extrapolation. As indicated, the function f depends on unknown parameters θ that are to be estimated. In general, the mapping also depends on certain hyperparameters denoted Υ , which must be carefully specified a priori, before estimation of θ . The term ϵ represents noise, a residual stochastic component of the model.

In applications of machine learning to nuclear physics, the primary goal is reliable extrapolation from the existing database of a given nuclear property, i.e., *generalization*, rather than a precise representation of the training data itself. With generalization the dominant consideration, the complexity of the model must be controlled as well as optimized, seeking the best compromise between simplicity and flexibility. This is the model selection problem.

If the model is too simple or inflexible, it may not fit the data well enough, resulting in poor predictive power. Conversely, if it is too flexible relative to the available training data, it is susceptible to overfitting of that data (which may be contaminated with spurious noise), at the expense of extrapability to new data regimes.

In other words, apart from choosing an appropriate machine-learning framework – for example, multilayer feedforward neural networks, radial basis function representations, support vector machines, Bayesian neural nets – the ability to find the right hyperparameters for the assumed statistical model can be crucial for its performance based on the existing data. Grid searches can be employed in seeking the most favorable combinations of hyperparameter values.

A valuable approach to controlling the complexity of a model, i.e., avoiding overparameterization, is regularization. This involves adding a penalty function to the assumed loss (or "cost") function (which is analogous to energy, being subject to minimization in optimization of the model). Scaling such a penalty term with an adjustable multiplicative parameter allows for control of the degree of regularization. In seeking a model having strong generalization capability, it must be expected that such a model will typically not give the smallest error with respect to the given training data. There is a natural trade-off between training error and generalization error.

The most straightforward approach to model selection is to evaluate the performance of model candidates on data independent of that used in training, which serves as a validation set. Using the original training set, one may generate as many such candidates as there are different combinations of model hyperparameters Υ (or a chosen subset of them). The models of this collection are then evaluated based on their performance on the validation set, the model with the best score being selected. Since there will still be some dependence between the chosen model and the assumed validation set, overfitting to this set may occur. Therefore the performance of the selected model should be confirmed by evaluating it on a third data set that is independent of both training and validation sets: the test set.

The validation process can be resource intensive. In practice, the quantity of data available may not permit the luxury of reserving a significant portion for model selection. In such cases, \mathcal{X} -fold cross-validation provides an alternative. The training data is partitioned randomly into \mathcal{X} approximately equal subsets. Considering in turn each of these subsets as the validation (or "holdout") set and the remaining $\mathcal{X}-1$ subsets as comprising the training

set, a validation score is assigned to the resulting model. The completed process yields \mathcal{X} competing models, and the final cross-validation error is determined from the mean validation score over the \mathcal{X} decompositions. Typical choices of \mathcal{X} are 5 to 10. Before computing the generalization error, the selected model is retrained using the *full* training set.

3. MULTILAYER PERCEPTRONS (MLP) AND THEIR TRAINING

The artificial neural network learning algorithm adopted for our study of α decay of heavy nuclei is based on the feedforward multilayer perceptron architecture sketched in Fig. 1, consisting of an input layer, an output layer, and one or more intermediate ("hidden") layers, each composed of "nodes" or neuron-like units. Information flows exclusively from input to hidden to output layers. For simplicity, we consider here only one hidden layer, consisting a number J of nodes j that serves as a hyperparameter. (Generalization to multiple hidden layers is straightforward). Ordinarily, every node in a given layer provides input to every node in the succeeding layer, with no reciprocal connections; in this respect the network is fully connected.

The input layer is composed of I nodes i that serve only as registers of the activities x_i of each input pattern. However, the J nodes j of the hidden layer and the K nodes k of the output layer process, in turn, their respective inputs x_i and h_j in a manner typically analogous to biological neurons. This produces corresponding outputs $h_j = f(b_j + \sum_i w_{ji}x_i)$ and

$$y_k = b_k + \sum_j w_{kj} h_j \tag{2}$$

in terms of IJ + JK connection weights plus J + K bias parameters: collectively $w = \{w_{ji}, w_{kj}\}$ and $b = \{b_j, b_k\}$. For the application reported here, the activation (or "firing") function f of processing units in the middle layer was chosen as $f(u) = \tanh(u)$, resembling the response of biological neurons.

Here we must note that because regression is the main task to be performed in our application, the outputs are not required to lie in any particular interval. Accordingly, outputs of the network are better computed as linear combinations of the outputs of the hidden layer plus a bias. This is the same as not considering any activation function in the output layer.

The collection w of weights of the connections from input to hidden units and from the hidden units to the output units, together with the biases b of these units, determine the given MLP as a proposed solution of the regression problem represented by Eq. (1). In the backpropagation learning algorithm, the weights are commonly optimized by gradient-descent minimization of the loss function

$$L(w,\lambda) = \frac{1}{2} \sum_{n=1}^{n_T} [y_n - f(x_n, w)]^2 + \frac{1}{2} \lambda ||w||^2,$$
 (3)

which is constructed from a sum of squares of output errors for the n_T examples provided by the training set, plus a simple regularization term that punishes weights of large magnitude. In our implementations of gradient descent, large weight oscillations are discouraged by a "classical" momentum term [20] in each training step s, according to

$$\Delta w_s = -\alpha \nabla L(w_{s-1}) + \mu \Delta w_{s-1} \tag{4}$$

(or alternatively with Nesterov's momentum [21]). Here ∇L_w denotes the gradient of the loss function evaluated at w_s , while $0 < \alpha < 1$ is the learning rate and $0 \le \mu < 1$ is the momentum parameter. (Also implemented in our applications are adaptive moments ("Adam") [22], involving moving averages of gradient and squared gradient, bias correction for second moments, and associated weight updating.)

We refer the reader to the standard texts [23–25] for more thorough and authoritative introductions to neural networks and machine learning.

4. SPECIALIZATION TO MACHINE LEARNING (ML) OF ALPHA DECAY

In our exploratory study, we focus attention on one specific application of ML to statistical modeling and prediction of nuclear properties, namely α -decay lifetimes of heavy nuclei, based on the multilayer perceptron procedures outlined in the preceding section. Additionally, some results of alternative strategies for exploration of the same problem domain will be summarized.

For this ML application, the data involved in both ML statistical modeling and assessment of the theoretical model chosen as reference include:

(i) The experimental half-lives $T_{1/2}^{\text{exp}}$ (measured in seconds) of a set of 150 nuclear isotopes (N, Z) with $Z \ge 104$.

(ii) Corresponding experimental values of the energy release $Q_{\alpha}(Z, N)$, which is M(Z, N) - M(Z-2, N-2) - M(2, 2) in terms of reactant masses.

These data sets, assembled from Refs. [15, 16], contain entries for the 120 neutron-deficient nuclides in Table I of Ref. [16], supplemented by entries for the 30 non-overlapping nuclides with Z = 80 - 118 drawn Table I of Ref. [15]. (Sources for the experimental values are cited in these two studies; such values and their uncertainties may differ from those provided by the National Nuclear Data Center.) Fig. 2 displays plots of the experimentally determined $\log T_{1/2}$ values versus Z, N, A, and input Q_{α} , for the composite data set of 150 nuclides.

Inputs to the MLP network models include Z, N, their parities, and their distances d_Z and d_N from respective proton and neutron magic numbers, viz. 2, 8, 20, 28, 50, 82, and 126 for Z, plus 184 for N, for a total of 7 inputs, including the experimental Q_{α} values.

As is conventional in modeling of decay rates, the actual quantity targeted is the base-10 logarithm $t = \log_{10} T_{1/2}$ of the half-life $T_{1/2}$. For a given model of the half-life data (whether theoretical or statistical), the key figure of merit is the smallness of the standard deviation

$$\sigma = \frac{1}{n_T} \left[\sum_{n=1}^{n_T} (t_n^{\text{exp}} - t_n^{\text{mod}})^2 \right]^{1/2}$$
 (5)

of the model estimates from experiment. If the ML procedure is used in the alternative mode of modeling the differences between a given theoretical model (th) and experiment (exp), so as to develop a statistical model of the "residuals" (res), the second term within the parentheses in Eq. 5 is replaced by $-t_n^{\text{th}} - t_n^{\text{res}}$.

Inputs to the neural network model, I = 7 in total, consist of the atomic and neutron numbers Z and N, their parities, the decay energy Q_{α} , and the distances $|Z - Z_m|$ and $|N - N_m|$ of a given input nuclide from the nearest respective magic numbers (viz. 8, 20, 28, 50, 82, 126 for protons, plus 84 for neutrons).

For model assessment, the full data set was randomly split into:

- (i) A training set (TR), comprised of 80% of the data (120 nuclear "patterns".
- (ii) A test set (TS), 20% of the data (30 patterns), provided by the remainder.

Model selection was carried out by five-fold cross-validation, as explained in the preceding section. A total of 2750 combinations of $(J, \lambda, \alpha, \mu)$ values (i.e. number of hidden units, regularization strength, learning rate, and momentum) were compared. The specific learning

algorithm applied was gradient descent with Nesterov's momentum. The number of epochs (passages through the training data) was 3000. Batch updating (batch size = 32) was applied, with data shuffling. During the learning phase, the quality measure σ was monitored at each epoch. Weights/biases were chosen to minimize $\sigma(TR)$ over epochs. These network parameters were then used to make predictions for new nuclear examples, outside the training set.

Two kinds of network model were constructed:

- (i) Net1: Trained on the experimental half-life data for the selected 150 nuclear examples drawn from Refs. [15, 16], yielding a purely statistical model of α decay. Fig. 3 provides different visualizations of the training and test sets used for this network model.
- (ii) **Net2**: Trained on the data set consisting of the differences between the predictions of a given theoretical model of α decay (specifically, ELDM), providing statistically derived corrections to this model.

After finding the best combination $(J^*, \lambda^*, \alpha^*, \mu^*)$ of hyperparameters for **Net1** and **Net2**, the most favored nets were trained again, but now using the whole set of training data at once.

5. RESULTS FOR LEARNING AND PREDICTION

Table 1 summarizes the results of these machine-learning procedures applied to α -decay half-life data for the 150 heavy nuclei extracted from Refs. [15, 16]. Optimal sets of the parameters $(J, \lambda, \alpha, \mu)$ are shown for the two network models, along with the respective quality measures σ attained by these nets on training, validation, and test sets, respectively denoted TR, VS, and TS. Corresponding values of the standard-deviation quality measure σ as achieved with the theoretical models employed by Cui et al. in these references are entered for comparison. Fig. 4 gives a schematic view of the quality of prediction achieved by **Net1** and **Net2**. Fig. 5 provides more refined graphical representations of the performance of **Net2** on training and test sets.

Table 1. Summary of machine-learning results for the quality measure σ , compared with corresponding results from the theoretical models applied in Refs. [15, 16]. Also displayed are the optimal parameter choices used for the ML models.

Predictor	$\sigma(TR)$	$\sigma(VS)$	$\sigma(TS)$	$(J^*, \lambda^*, \alpha^*, \mu^*)$
ELDM	0.5690	_	0.5845	_
Net1	0.4468	0.5073	0.4910	$(4, 10^{-1}, 10^{-3}, 0.99)$
Net2	0.4586	0.4756	0.4773	$(20, 1, 10^{-3}, 0.99)$

CONCLUSIONS AND OUTLOOK

Table 1 shows a modest reduction of the error measure σ of the theoretical models upon implementing machine learning, although it is clear that ML is quantitatively competitive with the best of current quantum-mechanical models of α decay. It is significant, however, that quite unlike what is found in ML of nuclear masses [1, 2] there is no appreciable improvement relative to the performance of the purely statistical ML model provided by Net1, when machine learning is applied to create Net2 by training only on the residuals of the chosen theoretical model.

There are several possible explanations for these findings. A major consideration is the paucity of data compared to the machine learning of nuclear masses. For α decay, the examples available for training are at most of order hundreds, whereas for masses there between two and three thousand measurements that may be used for training. It was for this reason that we chose to enlarge the α -decay data set of Ref. [16] by adding non-overlapping examples from the data set of Ref. [15]. This may have been counterproductive in that all of the added nuclei have Z > 104, whereas the data set of Ref. [16] is made up of neutron-deficient nuclei. More broadly, the irreducible sparsity of training data increases the danger of overlearning and accentuates the sacrifices made in its avoidance.

These considerations would not be so serious were it not for the fact that the experimental measurements of α and β decay rates are subject to relatively large errors compared to masses. This is responsible for the accepted rule-of-thumb that α -decay half-life predictions (measured in seconds) within an order of magnitude of the true value are considered acceptable (cf. the "hindrance factor"). The clear implication is that in ML applications to nuclear decay, the learning algorithm should give explicit consideration to the noisy component of the data, to the extent it is quantifiable. A straightforward modification of the backpropagation algorithm to cope with this situation has been developed and tested in Ref. [26], and will be implemented in further ML treatments of α decay.

The otherwise unexpected results of an additional experiment carried out as a limiting case are relevant to the situation described. We sought to answer the question: How well does a degenerate version of the network model considered here, i.e., the Elementary Perceptron, perform on the alpha-decay problem? The answer is contained in Table 2, where **Net1** and **Net2** now have only a single processing layer (the output layer).

Table 2. Performance of the Elementary Perceptron in learning and prediction of alphadecay half-lives (cf. Table 1). Also displayed are the optimal parameter choices used for the ML models.

Predictor	$\sigma(TR)$	$\sigma(VS)$	$\sigma(TS)$	$(J^*,\lambda^*,\alpha^*,\mu^*)$
				$(0, 0, 10^{-2}, 0.0)$
Net2	0.4399	0.4837	0.4638	$(0, 0, 10^{-2}, 0.99)$

These results are not inconsistent with the above discussion. In the context of the alphadecay machine-learning problem where uncertainties in measured half-lives are large, course data can be modeled just as well by a course model.

ACKNOWLEDGMENTS

JWC expresses his gratitude for the hospitality of the University of Madeira during extended residence, and continuing support from the McDonnell Center for the Space Sciences.

J. W. Clark, S. Gazula, in Condensed Matter Theories, Vol. 6, S. Fantoni, S. Rosati, eds. (Plenum, New York, 1991), pp. 1-24; S. Gazula, J. W. Clark, H. Bohr, Nucl. Phys. A 540, 1 (1992); K. A. Gernoth, J. W. Clark, J. S. Prater, H. Bohr, Phys. Lett. B 300, 1 (1993); K. A. Gernoth, J. W. Clark, Neural Networks 8, 291 (1995); J. W. Clark, T. Lindenau, M. L. Ristig, Scientific Applications of Neural Nets (Springer, Berlin, 1999); Springer Lecture Notes in Physics, Vol. 522; J. W. Clark, K. A. Gernoth, S. Dittmar, M. L. Ristig, Phys. Rev. E 59, 6161 (1999); J. W. Clark, H. Li, Int. J. Mod. Phys. B 20, 5015 (2006), arXiv: nucl-th/0603037; S. Athanassopoulos, E. Mavrommatis, K. A. Gernoth, J. W. Clark, in Advances in Nuclear Physics, Proceedings of the 15th Hellenic Symposium on Nuclear Physics, G. A. Lalazissis, Ch. C. Moustakidis, eds. (Art of Text Publishing & Graphic Arts Co., Thessaloniki, 2006),

- pp. 65-70, arXiv: nucl-th/0511088; N. Costiris, E. Mavrommatis, K. A. Gernoth, J. W. Clark, Phys. Rev. C 80, 044332 (2009), arXiv:nucl-th/0806.2850; N. J. Costiris, E. Mavrommatis, K. A. Gernoth, J. W. Clark, arXiv:nucl-th/1309.0540; S. Akkoyun, T. Bayram, S. O. Kara, A. Sinan, J. Phys. G: Nucl. Part. Phys. 40, 055106 (2013); T. Bayram, S. Akkoyun, S. O. Kara, Ann. Rev. Nucl. Energy 63, 172 (2014); T. Bayram, S. Akkoyun, S. O. Kara, Journal of Physics: Conference Series 490, 012105 (2014).
- [2] R. Utama, J. Piekarewicz, H. B. Prosper, Phys. Rev. C 93, 1 (2016); R. Utama, J. Piekarewicz, Phys. Rev. C 97, 1 (2018).
- [3] H. F. Zhang, L. H. Wang, J. P. Yin, P. H. Chen, H. F. Zhang, J. Phys. G: Nucl. Part. Phys. 44, 045110 (2017).
- [4] G. A. Negoita, J. P. Vary, G. R. Luecke, P. Maris, A. M. Shirokov, I. J. Shin, Y. Kim, E. G. Ng, C. Yang, M. Lockner, G. M. Prabhu Phys. Rev. C 99, 054308 (2019).
- [5] L. Neufcourt, Y. Cao, W. Nazarewicz, F. Viens, Phys. Rev. C 98, 1 (2018), arXiv:1806.00552.
- [6] Z. M. Niu, H. Z. Liang, B. H. Sun, W. H. Long, Y. F. Niu, Phys. Rev. C 99, 064307 (2019).
- [7] J. H. Hamilton, S. Hofmann, Y. T. Organessian, Ann. Rev. Nucl. Part. Sci. 63, 383 (2013).
- [8] V. E. Viola, G. T. Seaborg, J. Inorg. Nucl. Chem. 28, 741 (1966).
- [9] G. Royer, Nucl. Phys. A 848, 279 (2010).
- [10] V. Yu. Denisov, A. A. Khkudenko, Phys. Rev. C 79 054614 (2009); 82, 059901(E) (2010).
- [11] G. Royer, B. Remaud, J. Phys. G: Nucl. Part. Phys. 8,
- [12] J. P. Cui, Y. L. Zhang, S. Zhang, Y. Z. Wang, Int. J. Mod. Phys. E 25, 1650056 (2016).
- [13] M. Goncalves, S. B. Duarte, Phys. Rev. C 48, 2409 (1993).
- [14] S. B. Duarte, O. Rodriguez, O. A. P. Tavares, et al., Phys. Rev. C 57, 2516 (1998).
- [15] J. P. Cui, Y. L. Zhang, S. Zhang, Y. Z. Wang, Phys. Rev. C 97, 014316 (2018).
- [16] J. P. Cui, Y. Xiao, Y. H. Gao, Y. Z. Wang, Nucl. Phys. A 987, 99 (2019).
- [17] K. P. Santhosh, C. Nithya, H. Hassanabadi, D. T. Akrawy, Phys. Rev. C 98, 024625 (2018).
- [18] T. Bayram, S. Akkoyun, S. O. Kara, Journal of Physics: Conference Series 490, 012105 (2014).
- [19] U. B. Rodriguez, C. Z. Vargas, M. Gon(c) alves, S. Barbosa Duarte, Fernando Guzma'n, J. Phys. G: Nucl. Part. Phys. 46, 115 (2019).
- [20] N. Qiang, Neural Networks 12, 145 (1999).
- [21] Y. Nesterov, Soviet Mathematics Doklady 27, 372 (1983).
- [22] D. P. Kingma, J. Ba, Adam: A method for stochastic optimization, International Conference

- on Learning Representations 2015, pp. 1-13, arXiv:1412.6980.
- [23] S. Haykin, Neural Networks and Learning Machines (Prentice Hall, New York, NY 2008).
- [24] C. M. Bishop, Neural Networks for Pattern Recognition (Oxford University Press, Birmingham, UK, 1995).
- [25] R. M. Neal, Bayesian Learning for Neural Networks, Lecture Notes in Statistics, Vol. 118 (Springer, New York, NY, 1996).
- [26] K. A. Gernoth, J. W. Clark, Computer Physics Communications 88, 1 (1995).

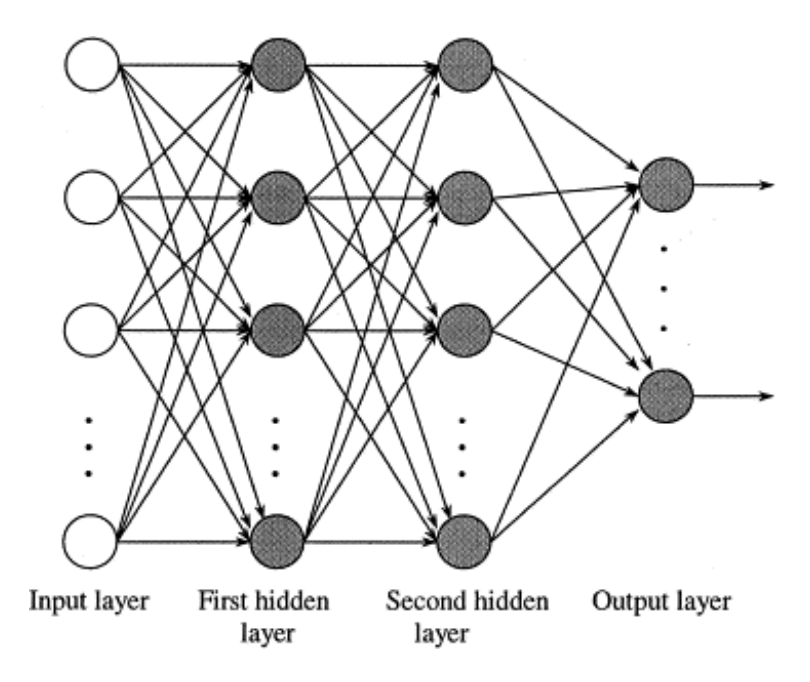


FIG. 1: Conventional multilayer feedforward neural network (Multilayer Perceptron) having two intermediate layers of "hidden neurons" between input and output layers. Darkened circles represent processing units analogous to neurons; lines oriented forward symbolize weighted connections between units analogous to interneuron synapses. Information flows left to right as units in each layer simulate those in the next layer.

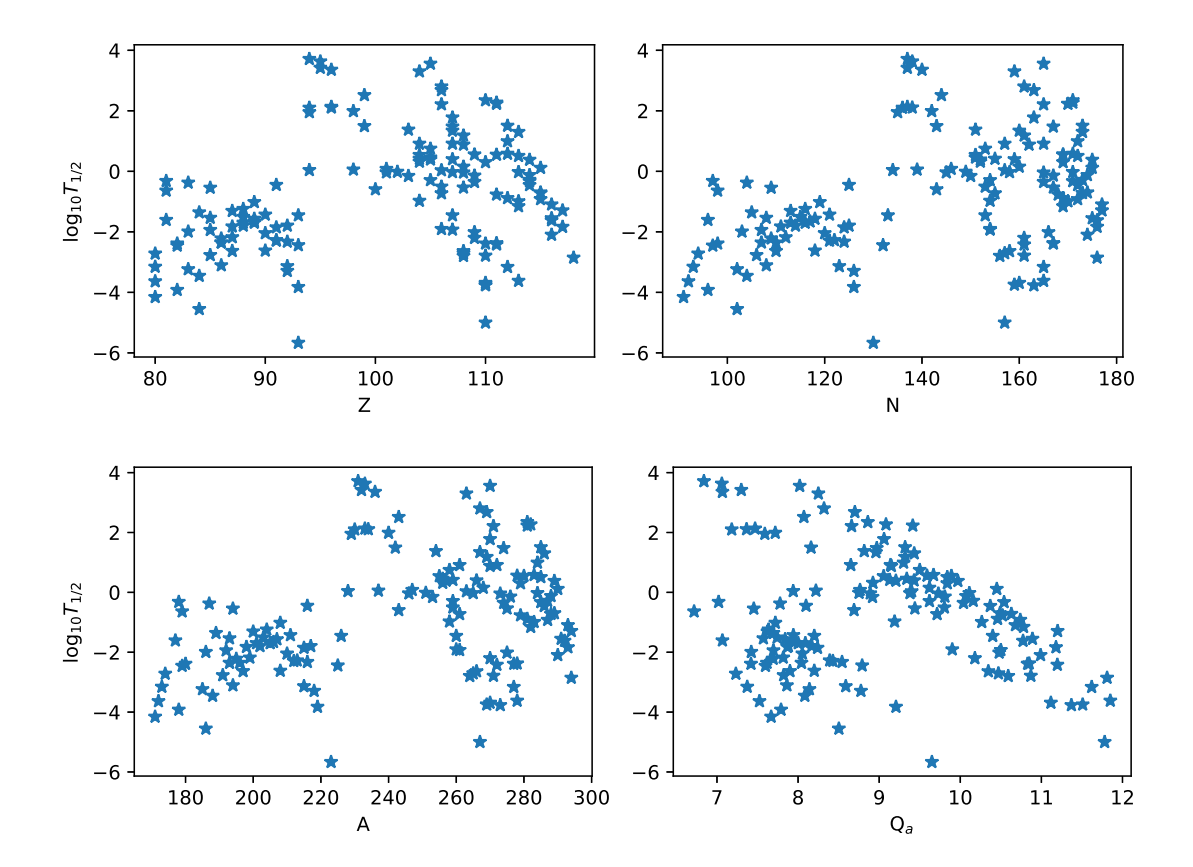


FIG. 2: Visualizations of measured experimental alpha-decay half-lives (in \log_{10} scale) for the 150 nuclei in the chosen database, plotted versus atomic number Z, neutron number N, mass number A, and energy release Q_{α} .

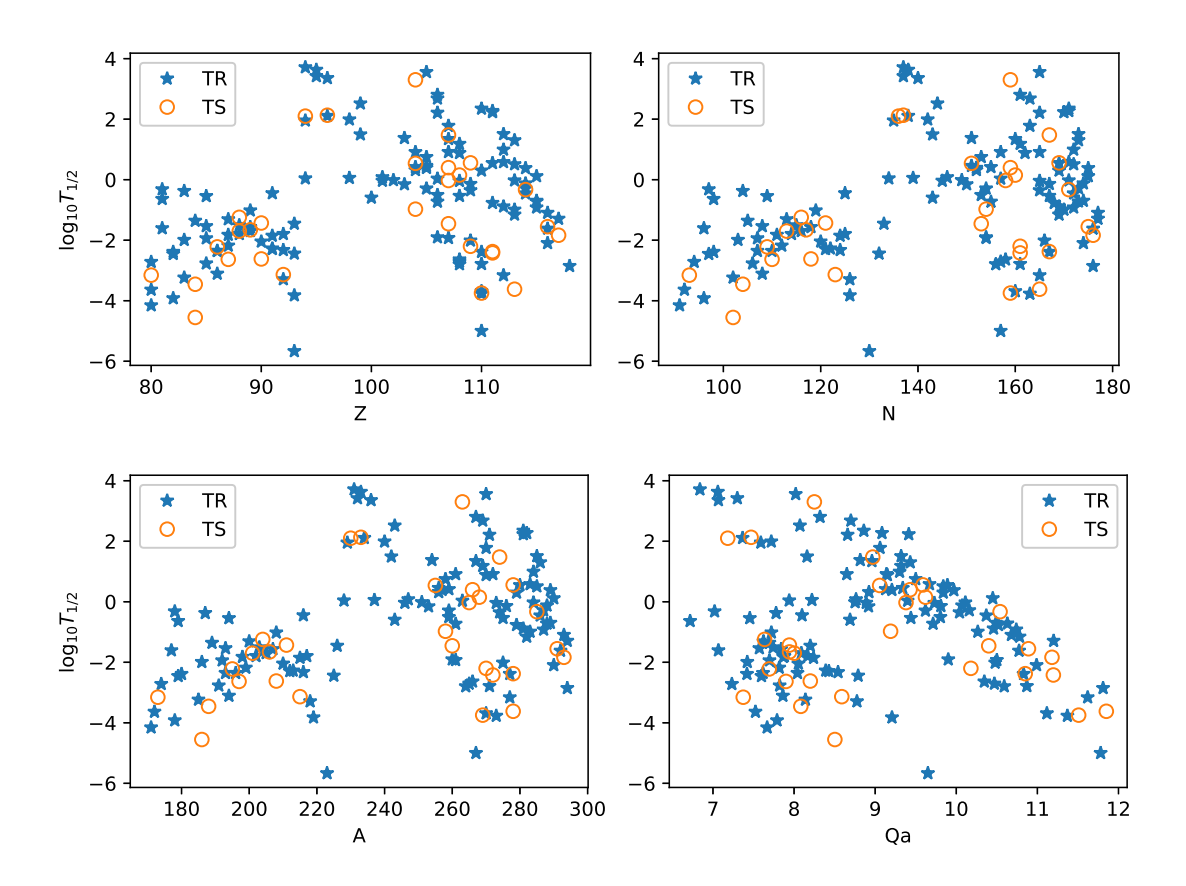


FIG. 3: Visualizations of the training set (TR) and test set (TS) adopted for **Net1**, plotted with respect to atomic number Z, neutron number N, mass number A, and energy release Q_{α} .

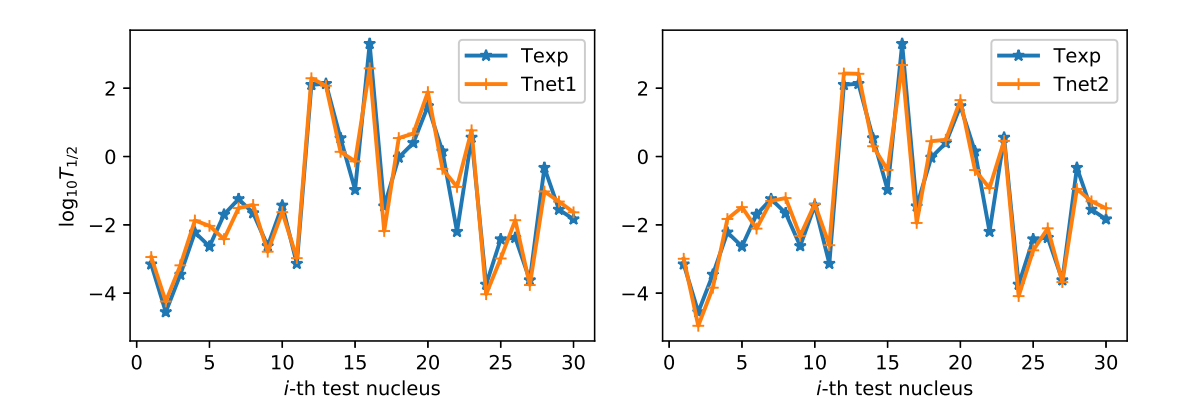


FIG. 4: Schematic representation of the performance of **Net1** and **Net2** in prediction of half-lives of test nuclides.

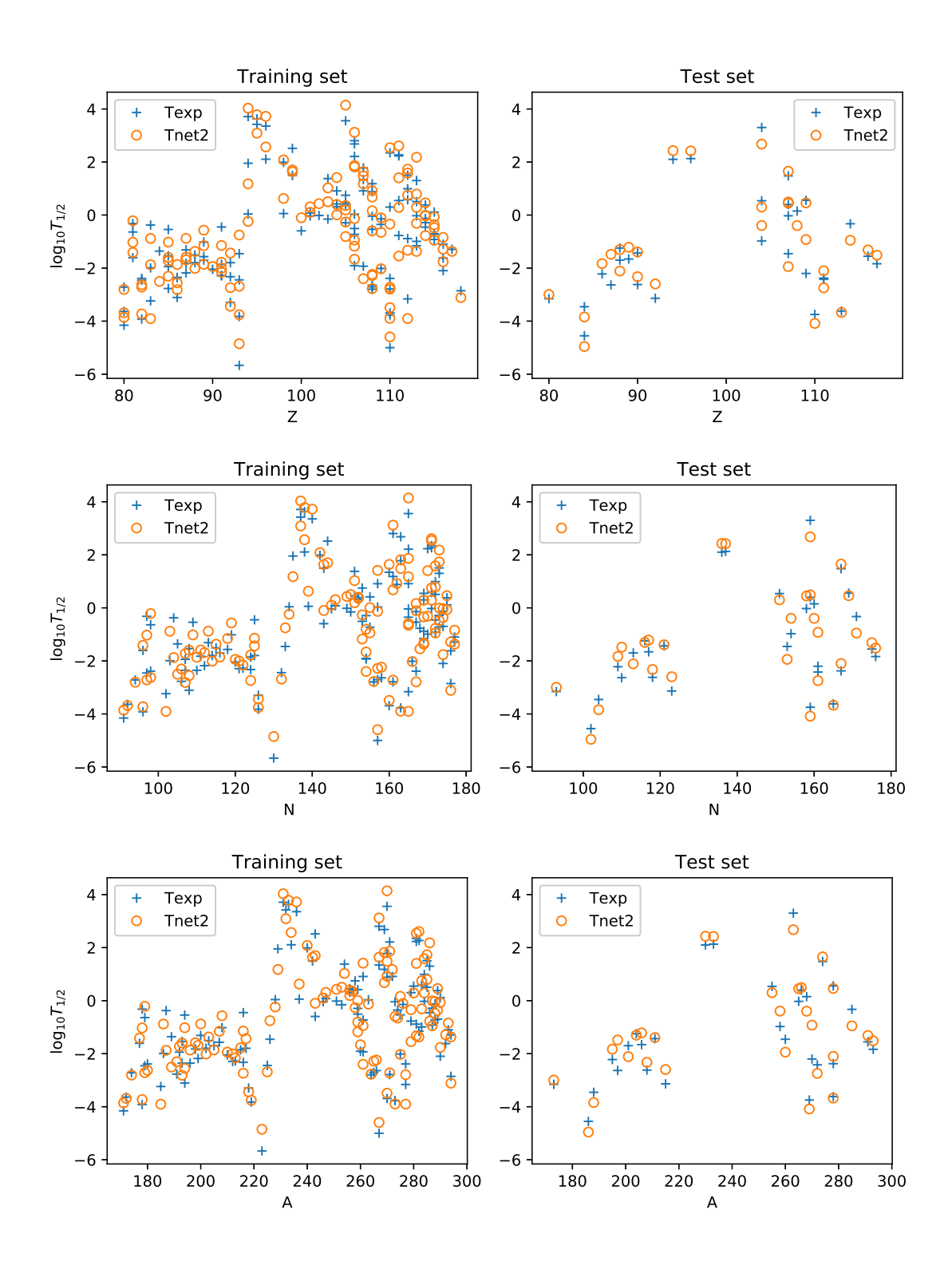


FIG. 5: Ensembles of half-life fits for training nuclei and predictions for test nuclei, generated by $\mathbf{Net2}$ and plotted versus atomic number Z, neutron number N, and mass number A.